applied sciences

MDPI

Article

Experimental Study on Effectiveness of a Prototype Seismic Isolation System Made of Polymeric Bearings

Tomasz Falborski * and Robert Jankowski

Faculty of Civil and Environmental Engineering, Gdansk University of Technology, 11/12 Narutowicza St., 80-233 Gdansk, Poland; jankowr@pg.gda.pl

* Correspondence: tomfalbo@pg.gda.pl; Tel.: +48-58-347-21-17

Received: 5 June 2017; Accepted: 3 August 2017; Published: 8 August 2017

Abstract: Seismic isolation is identified as one of the most popular and effective methods of protecting structures under strong dynamic excitations. Base isolators, such as Lead Rubber Bearings, High Damping Rubber Bearings, and Friction Pendulum Bearings, are widely used in practice in many earthquake-prone regions of the world to mitigate structural vibrations, and therefore minimize loss of life and property damage during seismic events. The present paper reports the results of the comprehensive experimental investigation designed to verify the effectiveness of a prototype base isolation system made of Polymeric Bearings in reducing structural vibrations. In order to construct seismic bearings considered in this study, a specially prepared polymeric material with improved damping properties was used. The dynamic behaviour of a single-storey and two-storey experimental model, both fixed-base and base-isolated, under a number of different ground motions, was extensively studied. The reduction in lateral response was measured by comparing the peak accelerations recorded at the top of the analyzed model structures with and without a base isolation system. The results of this research clearly demonstrate that the application of the prototype Polymeric Bearings leads to significant improvement in seismic response by reducing the lateral acceleration.

Keywords: polymeric bearings; base isolation; shaking table test; earthquakes; dynamic excitations; seismic performance

1. Introduction

Earthquakes are counted among the most severe and unpredictable threats to structures all around the world. Strong ground motions cause a lot of damage in a wide variety of ways, leaving sometimes thousands of casualties in their wake. The most frequently observed structural failures due to strong ground motions include soft-storey and weak-storey failures, brittle fracture and collapse of concrete and masonry structures, failures due to excessive plastic deformation in steel frame structures, pounding between adjacent buildings (see, for example, [1–3]), toppling of structures erected on soft and unstable soil, etc. During the last few years alone, the world has witnessed many major earthquakes, five of which have caused far-reaching consequences of a national scale for Haiti (January 2010), Chile (February 2010), New Zealand (February 2011), Japan (March 2011), and Turkey (October 2011). In spite of a number of available technical solutions to protect structures against seismic forces, earthquake peril remains the most sinister natural disaster for which many countries are still ill-prepared. Due to the randomness of occurrence, destructive potential, and insufficient early-warning systems, there is an incessant need for developing earthquake protection systems against seismic excitations and their devastating effects in order to enhance structural safety and reliability (see, for example, [4–6]).

It has been recognized that structures can be effectively protected against strong ground motions by various methods of structural control (see, for example, [7,8]). The general concept

of this design strategy is to modify structural dynamic properties, such as the fundamental period of vibration and the damping ratio, so that structures can respond more favourably to dynamic excitations (see, for example, [9–12]). The family of structural control methods has grown to include passive, active and hybrid (semi-active) systems (see, for example, [13]). Passive control (see, for example, [14,15]) is considered to be the safest approach, because, in contrast to active and hybrid devices (see, for example, [16]), no external source of energy is required to activate the system. Among passive control methods, base isolation is one of the most commonly employed strategies for protecting structures against earthquake forces (see, for example, [17–19]). It works by separating the structure from the horizontal components of the earthquake ground motion by introducing a layer with low horizontal stiffness between the superstructure and its foundation (see, for example, [20,21]). The main purpose of base isolation is to lengthen the fundamental period of vibration of the structure to reduce the base shear induced by the earthquake, while providing additional damping to the system (see, for example, [22]). Generally, base isolators can be grouped under laminated rubber bearings and sliding bearings. In the first approach, the isolation system introduces cylindrical or rectangular bearings with alternating layers of steel plates and hard rubber between the structure and its foundation (see, for example, [23]). In this approach, laminated rubber bearings are strong and stiff under vertical loads, and yet very flexible under lateral forces. One of the most popular devices of this type is the High Damping Rubber Bearing (HDRB). Because the natural damping of a standard rubber is relatively low, an additional damping can be introduced with the use of some sort of a mechanical damper (see, for example, [24,25]). A typical example is the Lead Rubber Bearing (LRB), which combines the laminated rubber bearing with a central lead core to improve the energy dissipation properties of the device (see, for example, [26–28]). Another type of isolation system uses rollers or sliders between the foundation and the base of the structure (see, for example, [29–32]). This approach assumes that a low level of friction reduces the transfer of shear across the isolation interface. The lower the coefficient of friction, the less shear is transmitted. However, in order to provide sufficient resistance to wind load and avoid unnecessary vibrations under small earthquakes, a fairly high value of frictional coefficient is required. The most popular sliding system that applies low frictional interfaces to reduce the transmission of shear force to the isolated structure includes Friction Pendulum Bearings (FPB).

At this point, it should be mentioned that base isolation is recognized to be most effective for structures with a fixed-base fundamental period of 1.0 s or less (e.g., low-rise and medium-rise buildings), and preferably erected on stiff and stable soils. Moreover, it should also be noted that the application of a seismic isolation system assumes that the structure will behave mainly in an elastic range, which may consequently result in a sub-exploitation of the building materials capacity. Therefore, this approach requires design procedures (specified, e.g., in building design codes and standards) that are slightly different from those traditionally utilized for the fixed-base buildings. Nevertheless, base isolators are widely used in practice in many earthquake-prone regions of the world and their effectiveness in protecting important structures during seismic events has been already confirmed (see, for example, [33,34]). However, the past few decades have witnessed tremendous progress in material engineering. Because of the impressive range of useful and exceptional properties, new materials may play an essential and ubiquitous role in many fields of science, including also earthquake engineering. The recent development of polymeric materials has resulted in an increased number of new applications and modifications of the existing ones.

Therefore, the present paper aims to verify experimentally the effectiveness of a prototype base isolation system made of the Polymeric Bearings (PBs), which are constructed with the use of a specially prepared polymeric material with improved damping properties. In order to achieve the above-mentioned aim of the current study, the following specific objectives have been established:

1. Perform an extensive material testing to determine the basic mechanical properties of the polymer used to construct the PBs;

2. Conduct the Dynamic Mechanical Analysis to evaluate the viscoelastic characteristics of the analyzed polymer over a wide range of temperatures for different excitation frequencies;
3. Design and construct a prototype base isolation bearing with the use of a specially prepared polymeric material;
4. Prepare two experimental models with different dynamic characteristics;
5. Investigate the dynamic behaviour of the structure models of both fixed-base and base-isolated during sine sweep testing;
6. Conduct an extensive shaking table testing to investigate the dynamic behaviour of the tested models with and without the PBs under various ground motions.

2. Material Testing

The material employed to construct the prototype PBs is a specially prepared flexible polyurethane-based elastomer. The chemical composition of this polymer includes certain additives to improve its damping properties, which are extremely desirable for energy-dissipation devices, particularly for seismic isolation bearings. The analyzed polymer has been used so far for the crack injections in the recently proposed Flexible Joint Method (FJM), which is an innovative technique of repairing damaged masonry and concrete structures. The effectiveness of the FJM in strengthening damaged structures has been confirmed through many in situ and laboratory tests, and the results obtained from both experimental and numerical studies have been already published (see [35]).

In order to get an insight into the basic mechanical characteristics of the analyzed polymer, an extensive material testing was firstly performed. The first stage was to conduct static tension and compression tests with the use of the polymeric cylindrical specimens measuring 28 mm in diameter and 28 mm high. For the purpose of this investigation, a Zwick/Roell Z020 mechanical tester (Zwick/Roell, Ulm, Germany) was employed. The measurements were performed in a room temperature of T = 23 °C, and relative humidity of 50% for five different strain rates: $v_1 = 10^{-1}\text{s}^{-1}$, $v_2 = 5 \times 10^{-2}\text{s}^{-1}$, $v_3 = 10^{-2}\text{s}^{-1}$, $v_4 = 5 \times 10^{-3}\text{s}^{-1}$, and $v_5 = 10^{-3}\text{s}^{-1}$. The tests were conducted until the total failure of the tested specimens. The average stress–strain curves from the static tension and compression tests are shown in Figure 1.

The results clearly demonstrate that the analyzed polymer is markedly nonlinear and its mechanical behaviour strongly depends on the strain rate, which is typical for viscoelastic materials. If the load is applied slowly, the stress relaxation occurs. On the other hand, if the load arises rapidly, the influence of relaxation phenomena on stress–strain behaviour is less significant. The strength of the tested material, which is a consequence of its modulus, appears to increase with the higher strain rate. Therefore, the higher the strain rate, the larger the force needed to obtain the same deformation level.

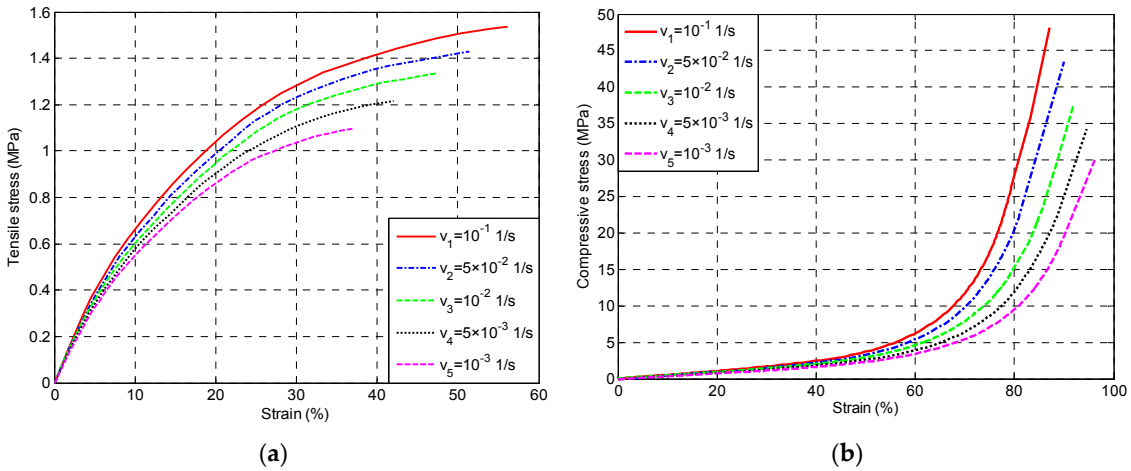

Figure 1. (**a**) Tensile and (**b**) compressive stress–strain curves for five different deformation rates.

In order to determine the dynamic properties of the analyzed polymer, Dynamic Mechanical Analysis (DMA) tests were performed. The DMA test is the most commonly adopted method to measure the viscoelastic parameters of various materials, as they are subjected to constant oscillating deformations over a wide range of temperatures. More specifically, when a sinusoidal load is applied, the resultant sinusoidal strain is measured. In this approach, phase difference between the stress and strain plots, together with the amplitudes of the stress and strain waves, are used to determine a variety of fundamental material parameters, including storage modulus, loss modulus, loss factor, and the glass transition temperature. The storage modulus represents the elastic behaviour of the material and defines the energy stored due to the applied strain. The loss modulus depicts the viscous behaviour of the material and defines its energy dissipation properties. The ratio of the loss to storage modulus, which can be calculated as the tangent of the phase angle between the stress and strain waves, is termed as the loss factor and provides the information on the relationship between the elastic and inelastic components. In addition, the loss factor is frequently used to characterize the damping properties of viscoelastic materials. The larger the tangent of the phase angle, the greater the energy dissipation ability of the material. Finally, the glass transition temperature, which is measured by the peak value of the tangent of the phase angle, separates two dramatically different states of deformation resistance. At temperatures below the glass transition temperature, the material is hard and brittle, whereas, at temperatures above the glass transition temperature, the material is more flexible and rubbery.

The DMA tests were carried out using TA Instruments Q800 Dynamic Mechanical Analyzer (TA Instruments, New Castle, DE, USA). The beam samples (60 × 10 × 4 mm) were clamped at one end (single cantilever mode) and subjected to constant oscillating deformations over a temperature range of −100 to 100 °C for four different excitation frequencies: 1, 2, 5, and 10 Hz. The excitation amplitude was set to 20 µm, and the heating rate to 3 °C/min. The plots of the storage modulus, loss modulus, and the tangent of the phase angle over a wide range of temperatures for four different excitation frequencies are shown in Figure 2.

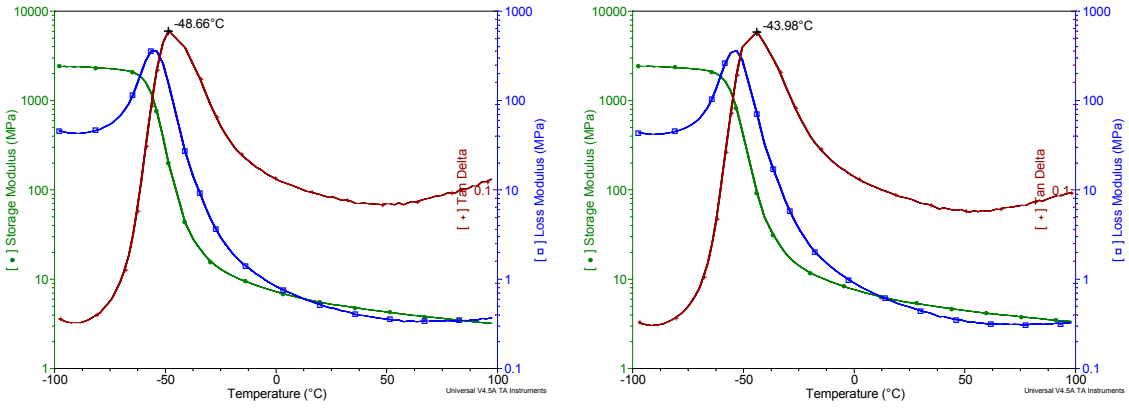

Figure 2. *Cont.*

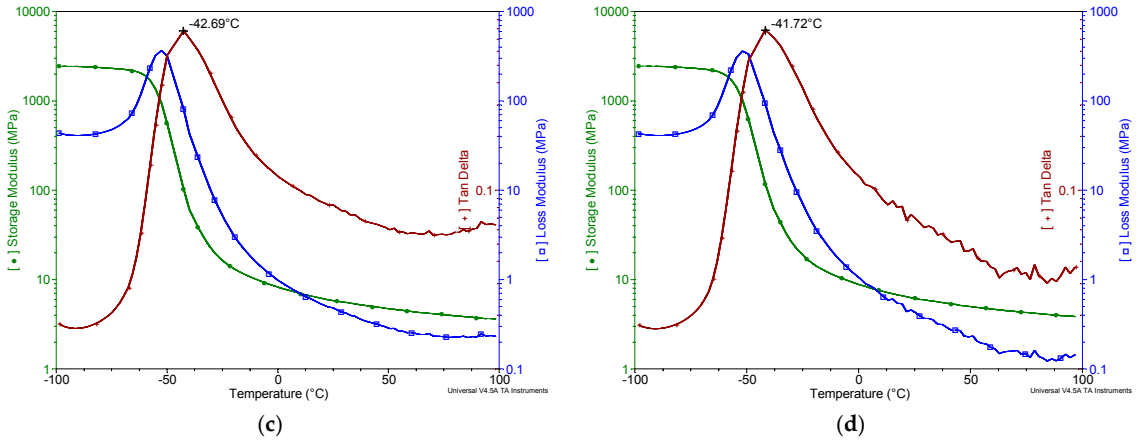

Figure 2. Dynamic mechanical analysis (DMA) results for various excitation frequencies: (**a**) 1 Hz, (**b**) 2 Hz, (**c**) 5 Hz, and (**d**) 10 Hz.

The glass transition temperature, usually denoted as T_g, which is one of the most significant parameters used to characterize mechanical behaviour of polymers, was measured by the peak value of tangent of the phase angle. As indicated in Figure 2, the exact values of T_g were determined for each of the analyzed excitation frequencies. It can be observed that T_g rises with the increasing excitation frequency, which is actually typical for viscoelastic materials due to molecular relaxation. In the glassy region (i.e., at temperatures $T < T_g$), the analyzed polymer is hard and brittle, so that its storage modulus is at its highest value, while the loss factor is generally low. In the transition region (i.e., at temperatures $T \cong T_g$), the analyzed polymer softens, as a result of which the material goes through its most rapid rate of change in stiffness and exhibits the highest level of loss factor. In the rubbery region (i.e., at temperatures $T > T_g$) the analyzed material is flexible, and consequently its stiffness and loss factor are at lower, but still satisfactory levels.

The results obtained from the DMA tests confirmed that the dynamic properties of the analyzed polymer are influenced by both temperature changes and the frequency rate of deformation. Nevertheless, as presented in Figure 3, in typical atmospheric temperature range (-20 to 40 °C), and for predominant earthquake frequencies ($1 \div 10$ Hz), its dynamic mechanical properties vary only slightly with changes in temperature and excitation frequency. As a consequence, the mechanical behaviour of the analyzed polymer is more stable and easier to predict. Most importantly, relatively high value of the loss factor confirms its high damping properties, which are crucial for the materials used for seismic isolation bearings.

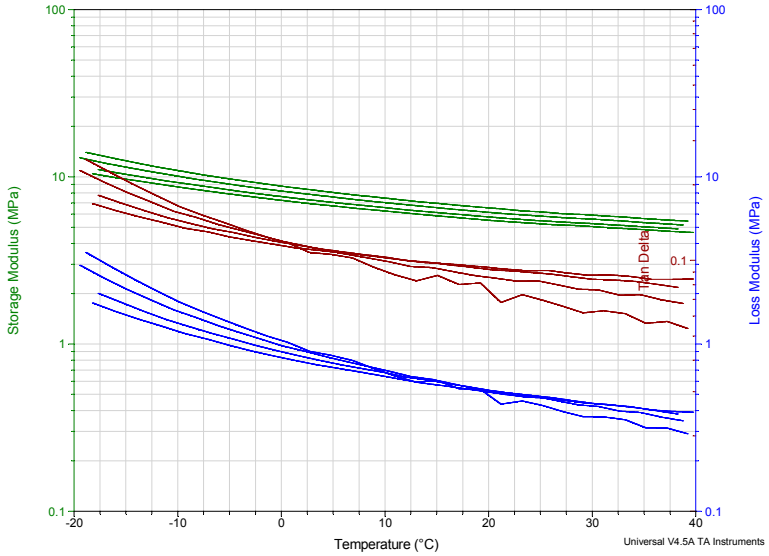

Figure 3. DMA results for all excitation frequencies in the temperature range from −20 to 40 °C.

3. Testing Conditions

3.1. Polymeric Bearings

A prototype PB considered in this research is made up of a polymer cylinder measuring 28 mm in diameter and 28 mm high with a centrally located hole (14 mm in diameter) into which a pin-ended steel core (6 mm in diameter) is inserted. Two additional steel anchor plates measuring 30 mm in diameter and 15 mm high were mounted at both ends of the polymer cylinder. The total height of the PB is 58 mm. The basic components of the prototype PB are shown in Figures 4 and 5. The prototype solution ensures that the steel core sustains vertical forces, while the polymer cylinder is subjected to shearing. In that way, the steel core prevents the polymer cylinder from carrying vertical loads that could possibly lead to undesirable bulging of the bearing. The maximum horizontal displacement of the PB is about 100% of its total height, which—when compared to HDRBs and LRBs—is a relatively high value. More importantly, the damping coefficient of the PBs calculated based on the experimentally obtained hysteresis loops ranges from 20% to nearly 50%, while, for most commonly used seismic isolators, the damping ratio is approximately from 10% to 20%.

It should be underlined that, due to uniaxial (horizontal) shaking table used in experimental study (see Section 3.2), the PBs were intentionally constructed as one-dimensional prototype devices capable to support only small experimental models. A full scale multi-dimensional version of the PB to be used for real structures has also been proposed and already submitted to the Polish Patent Department.

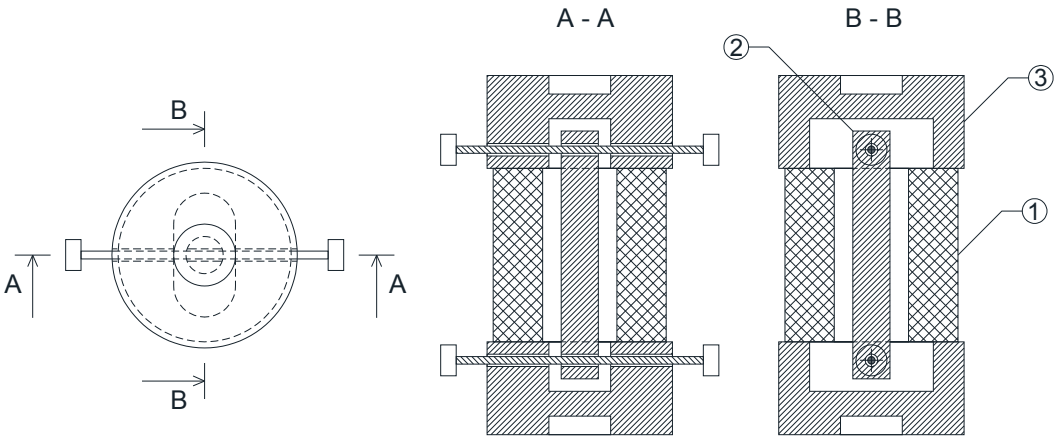

Figure 4. Technical sketch of the polymeric bearing (PB) (1: polymer cylinder with a centrally located hole, 2: pin-ended steel core, 3: anchor plate).

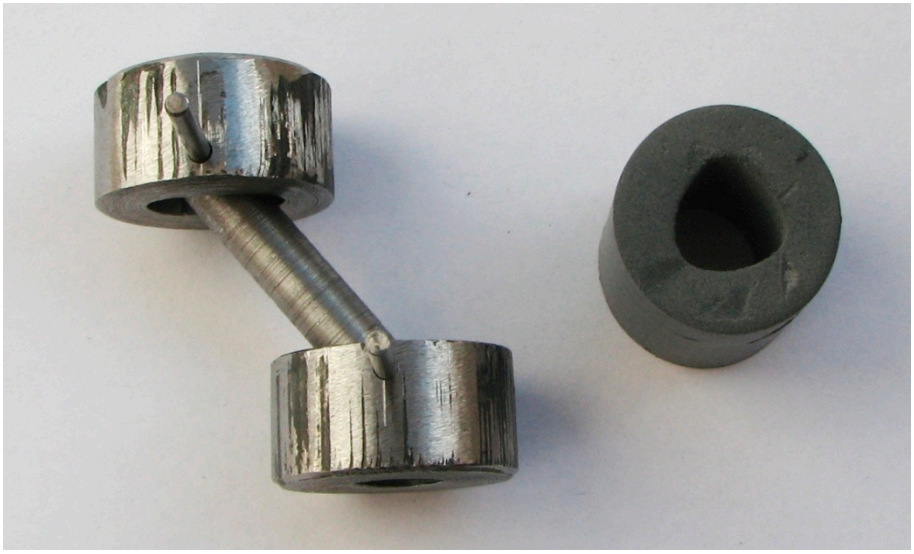

Figure 5. Components of the prototype PB: pin-ended steel core with the anchor plates (**left**), and a polymer cylinder with a centrally located hole (**right**).

3.2. Experimental Setup

An extensive shaking table test program was carried out to verify the effectiveness of the analyzed prototype base isolation system made of the PBs in improving dynamic behaviour of two experimental models. The investigation was conducted using a middle-sized one-directional shaking table, which was used to simulate the lateral forces and displacements caused by earthquake motions. The shaking table platform is 2 × 2 m and the lateral motion is powered by the linear actuator Parker ETB125 (Parker, Cleveland, OH, USA) with the stroke of 0.5 m and the maximum acceleration of 10 m/s^2. The experimental setup is shown in Figure 6.

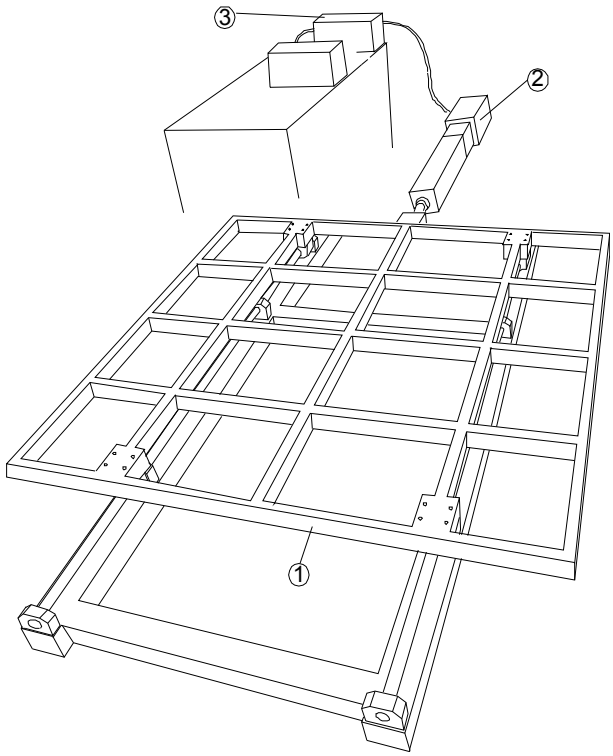

Figure 6. Technical sketch of the experimental setup (1: middle-sized shaking table platform, 2: linear actuator, 3: actuator controller).

3.3. Structure Models

In order to conduct the experimental investigation, a single-storey and two-storey structure models were prepared. The welded steel frames were constructed using the rectangular hollow section elements (RHS 15 × 15 × 1.5 mm). The columns were arranged in a rectangular pattern with spacing of 0.465 m in the longitudinal direction and 0.556 m in the transverse one. Diagonal bracing was used in the sidewall planes to counteract transverse and torsional vibrations. Moreover, concrete plates (50 × 50 × 7 cm) were employed to simulate the weight of the floor and foundation slabs. The welded steel frames were clamped together using M10 bolts. The single-storey structure model consisting of one steel frame and two concrete plates is 1.20 m high and weighs 95.12 kg, whereas the two-storey structure model consisting of two steel frames and three concrete plates is 2.30 m high and weighs 148.04 kg. The dynamic behaviour of these two experimental models, both fixed-base and base-isolated, was extensively studied during shaking table tests. The structure models with and without the PBs are shown in Figures 7 and 8.

Both single-storey and two-storey structure models have been specifically designed in order to accurately reflect the dynamic behaviour of real buildings. Therefore, the single-storey structure model, characterized by the fundamental frequency of 3.34 Hz, is representative for low-rise buildings, whereas the two-storey structure model, characterized by the fundamental frequency of 1.94 Hz, reflects the dynamic behaviour of medium-rise buildings.

(**a**) (**b**)

Figure 7. Fixed-base (**a**) and base-isolated (**b**) single-storey structure model.

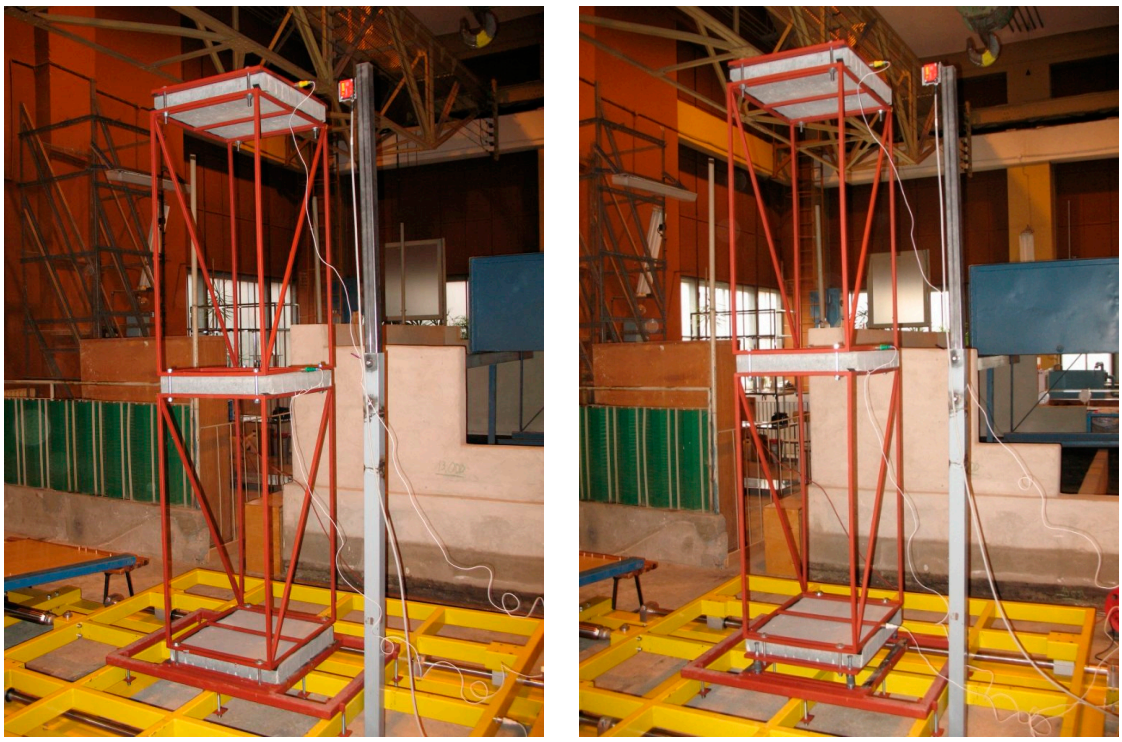

(**a**) (**b**)

Figure 8. Fixed-base (**a**) and base-isolated (**b**) two-storey structure model.

4. Sine Sweep Testing

The first step of the experimental investigation was the sine sweep testing. The structure models with and without the PBs were mounted on the shaking table and subjected to sinusoidal excitation with increasing frequency ranging from 0.1 up to 15 Hz. The tested models were instrumented with uniaxial

accelerometers to record the acceleration-time histories at different levels. The time-acceleration histories recorded at the top of the tested models are shown in Figures 9 and 10. In the case of the single-storey structure, the peak response acceleration is equal to 7.74 and 3.25 m/s^2 for the fixed-base and the isolated model, respectively. On the other hand, the peak response acceleration for the two-storey structure is equal to 4.42 and 2.44 m/s^2 for the fixed-base and the isolated model, respectively.

The results obtained clearly indicate that the application of the prototype PBs results in a considerable improvement of dynamic characteristics of the experimental models. Period elongation and additional damping associated with implementing PBs resulted in a significant decrease in lateral accelerations experienced by the tested models during sinusoidal excitation, which can be observed on the basis of time-acceleration histories presented in Figures 8 and 9. The reduction in peak lateral accelerations recorded at the top of the experimental models due to the application of the isolation devices was determined to be approximately 58% and 45% for the single-storey and two-storey structure models, respectively.

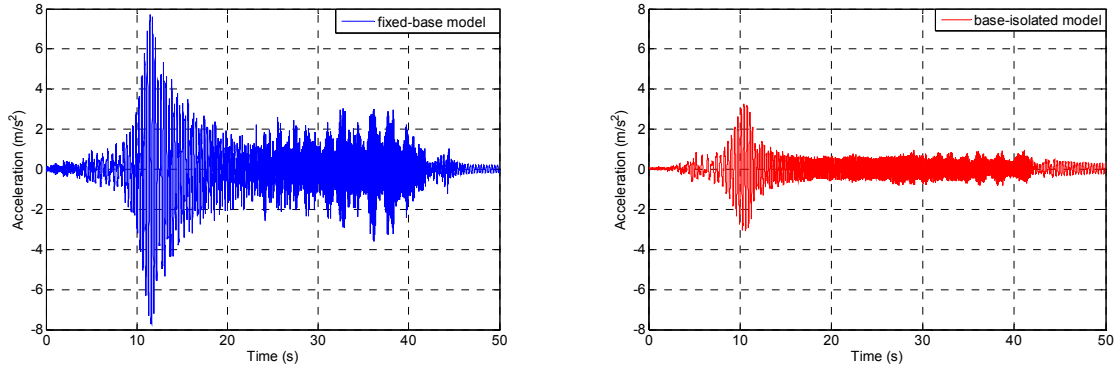

Figure 9. Time-acceleration history plots for the fixed-base (**a**) and base-isolated (**b**) single-storey model during the sine sweep test.

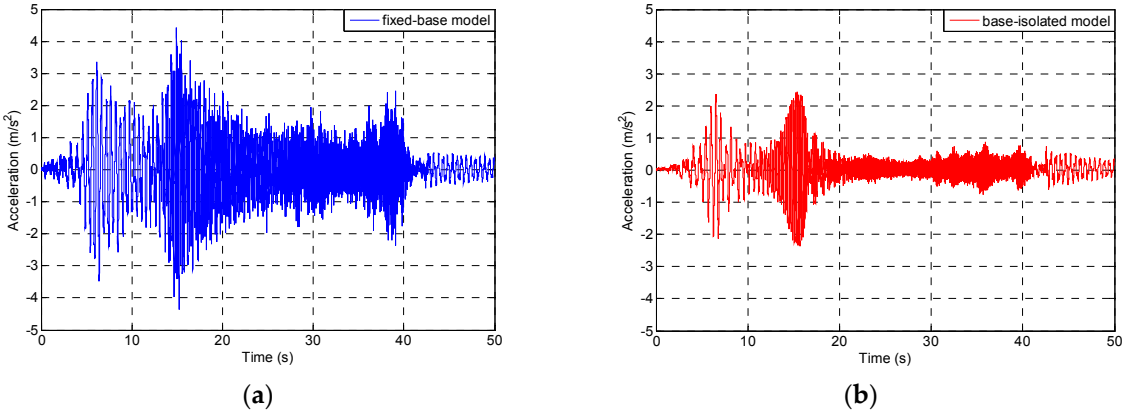

Figure 10. Time-acceleration history plots for the fixed-base (**a**) and base-isolated (**b**) two-storey model during the sine sweep test.

5. Shaking Table Testing

In the final stage of the experimental investigation, the dynamic behaviour of the structure models with and without the PBs under a number of dynamic excitations was extensively studied. The experimental models, both fixed-base and base-isolated, were subjected to the El Centro

earthquake of 1940, the San Fernando earthquake of 1971, the Loma Prieta earthquake of 1989, the Northridge earthquake of 1994, and finally the Polkowice (Poland) tremor of 2002 as an example of mining-induced seismicity, which is also a major concern of professional and research communities (see, for example, [36]). The tested models were instrumented with uniaxial accelerometers to record the acceleration-time histories at different levels. The effectiveness of the PBs in reducing structural vibrations under seismic excitations was verified by comparing the peak accelerations experienced at the top of the tested models. The time-acceleration history plots recorded at the top of the tested models are also shown in Figures 11 and 12. The peak accelerations recorded at the top of the analyzed single-storey and two-storey structure models, with and without the PBs, are briefly reported in Tables 1 and 2, respectively.

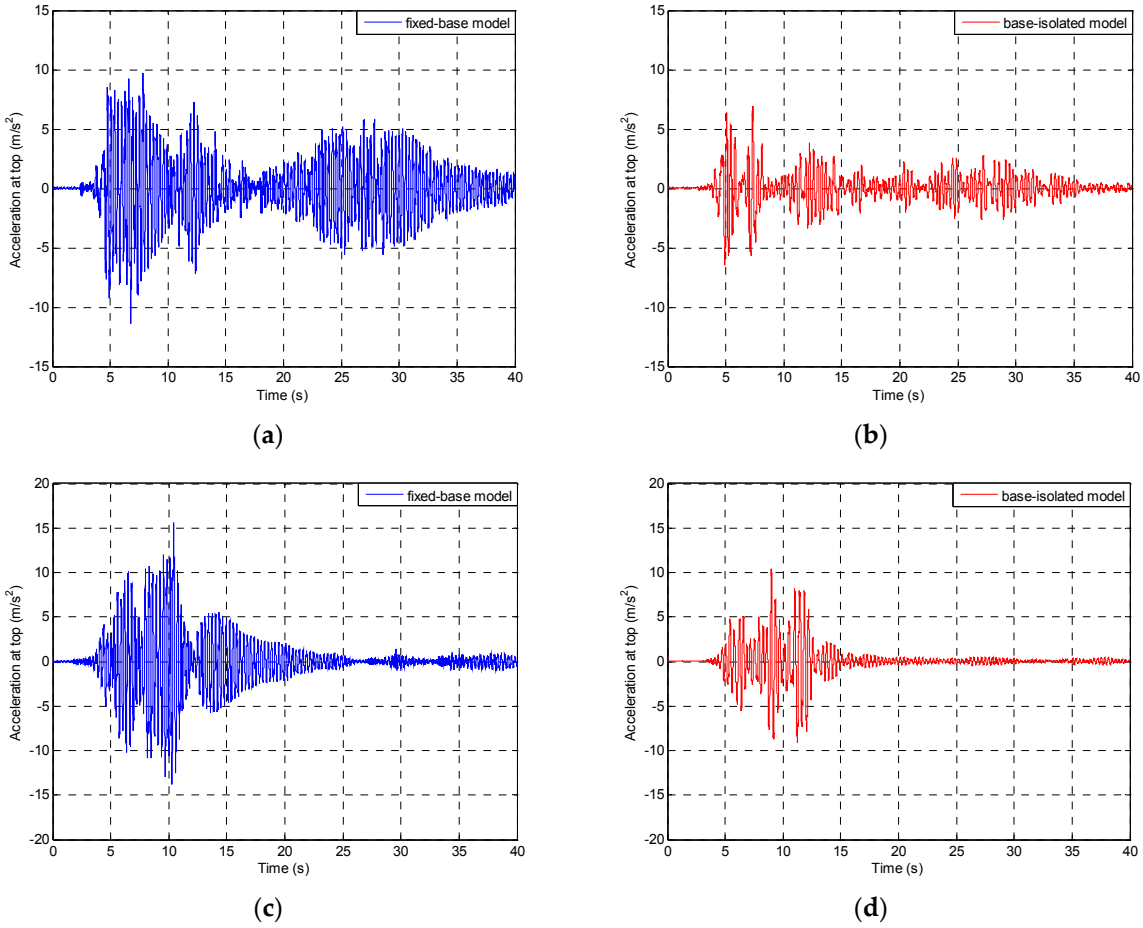

Figure 11. *Cont.*

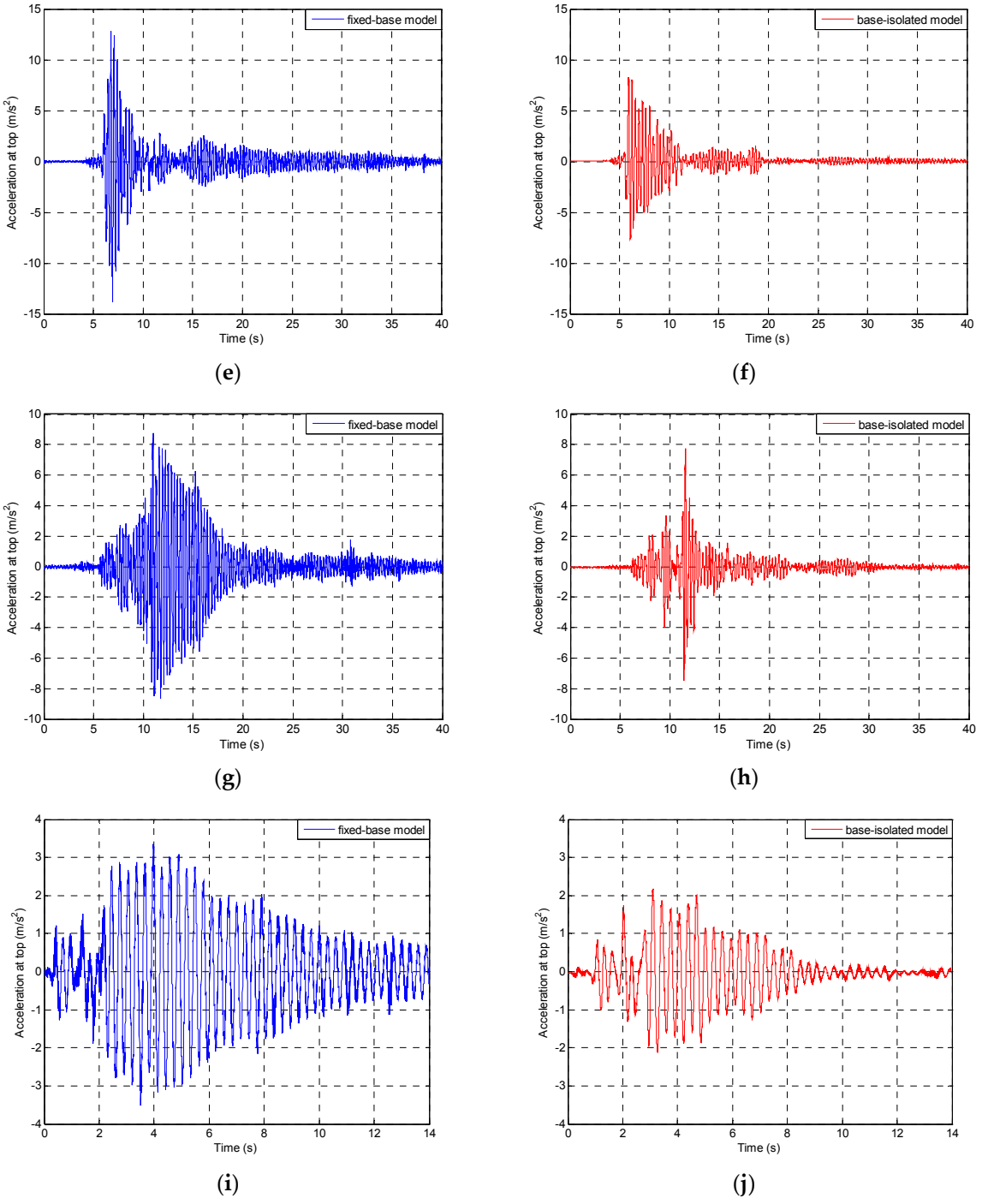

Figure 11. Time-acceleration history plots for the fixed-base (blue) and base-isolated (red) single-storey model during different earthquakes: the 1940 El Centro earthquake (**a**,**b**), the 1971 San Fernando earthquake (**c**,**d**), the 1989 Loma Prieta earthquake (**e**,**f**), the 1994 Northridge earthquake (**g**,**h**), and the 2002 Polkowice mining tremor (**i**,**j**).

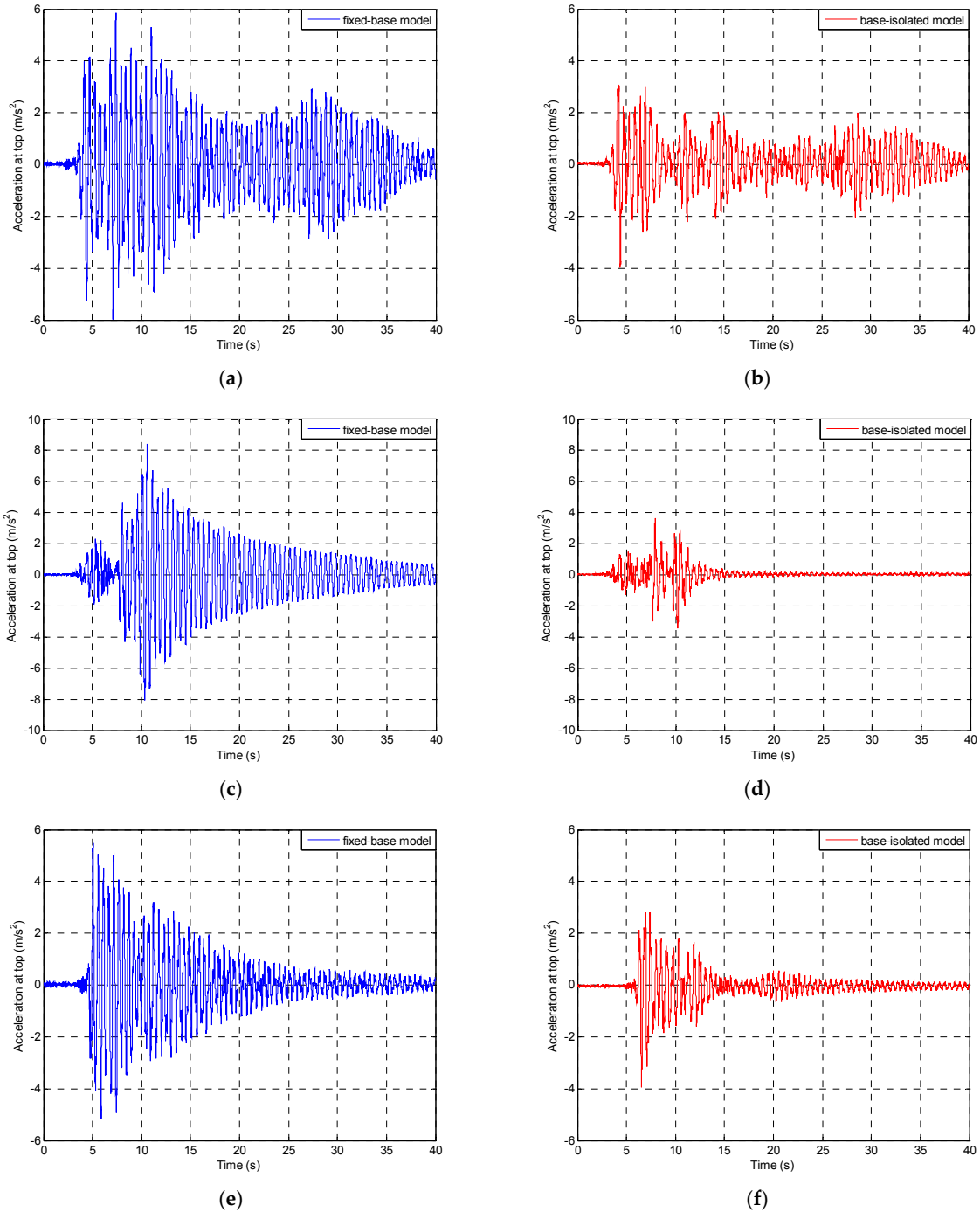

Figure 12. *Cont.*

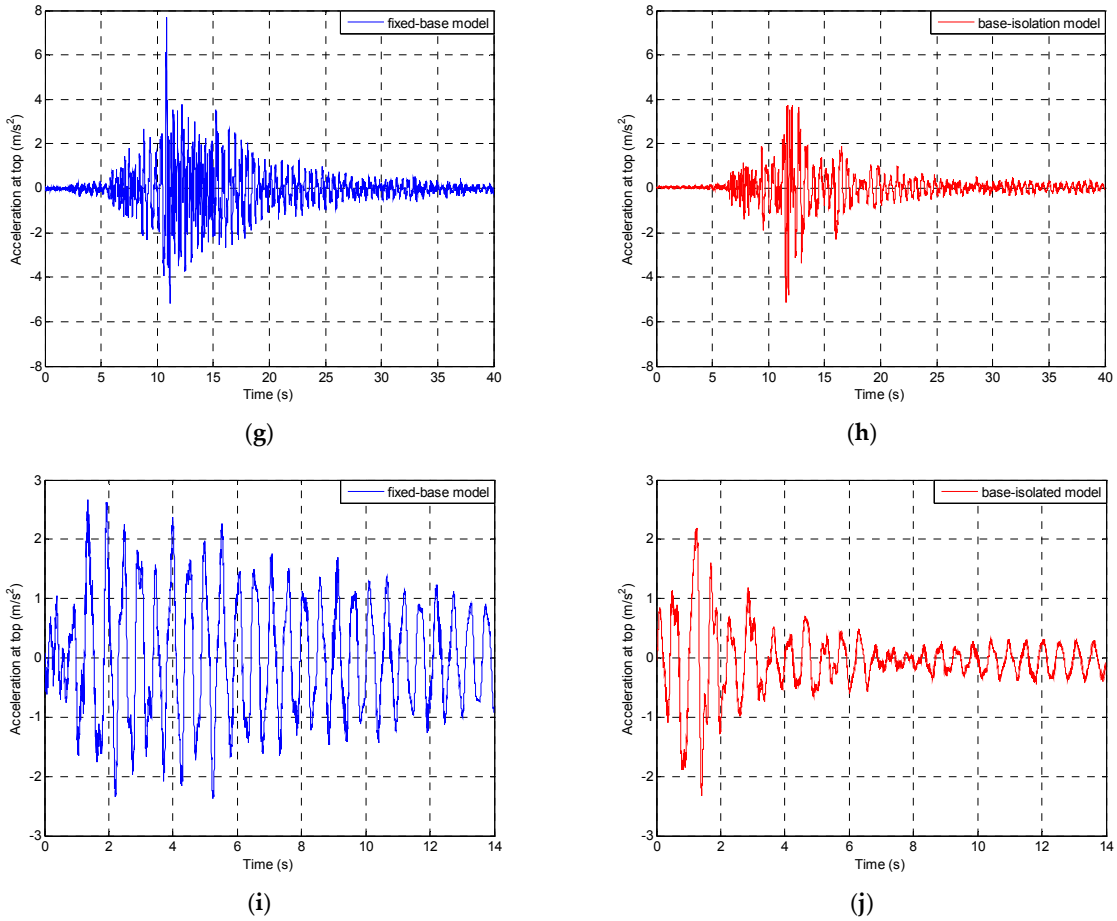

Figure 12. Time-acceleration history plots for the fixed-base (blue) and base-isolated (red) two-storey model during different earthquakes: the 1940 El Centro earthquake (**a**,**b**), the 1971 San Fernando earthquake (**c**,**d**), the 1989 Loma Prieta earthquake (**e**,**f**), the 1994 Northridge earthquake (**g**,**h**), and the 2002 Polkowice mining tremor (**i**,**j**).

Table 1. Results of the seismic tests for the single-storey structure model.

Dynamic Excitation	Peak Acceleration at the Top of the Tested Model (m/s^2)		Reduction (%)
	Fixed-Base Model	Model Isolated with PBs	
1940 El Centro earthquake NS component, original record with PGA = 3.070 m/s^2	11.39	6.98	38.7
1971 San Fernando earthquake Pacoima Dam station, N74°E component, scaled record with PGA = 5.688 m/s^2	15.59	10.47	32.8
1989 Loma Prieta earthquake Corralitos station, NS component, scaled record with PGA = 3.158 m/s^2	13.82	8.27	40.2
1994 Northridge earthquake Santa Monica station, EW component, scaled record with PGA = 4.332 m/s^2	8.73	7.74	11.3
2002 Polkowice mining tremor NS component, original record with PGA = 1.634 m/s^2	3.53	2.18	38.2

Where: PGA: Peak Ground Acceleration, NS: North-South, EW: East-West.

Table 2. Results of the seismic tests for the two-storey structure model.

Dynamic Excitation	Peak Acceleration at the Top of the Tested Model (m/s^2)		Reduction (%)
	Fixed-Base Model	Model Isolated with PBs	
1940 El Centro earthquake NS component, original record with PGA = 3.070 m/s^2	5.98	3.99	33.3
1971 San Fernando earthquake Pacoima Dam station, N74°E component, scaled record with PGA = 5.688 m/s^2	8.41	3.63	56.8
1989 Loma Prieta earthquake Corralitos station, NS component, scaled record with PGA = 3.158 m/s^2	5.49	3.95	28.1
1994 Northridge earthquake Santa Monica station, EW component, scaled record with PGA = 4.332 m/s^2	7.68	5.14	33.1
2002 Polkowice mining tremor NS component, original record with PGA = 1.634 m/s^2	2.67	2.34	12.4

Where: PGA: Peak Ground Acceleration, NS: North-South, EW: East-West.

The shaking table tests confirm very high effectiveness of the prototype base isolation system made of PBs in improving dynamic behaviour by reducing structural vibrations, thus enhancing structural safety and reliability. The inspection of Tables 1 and 2 demonstrates that, due the application of the isolation devices, the peak lateral accelerations recorded at the top of the tested structures were reduced by approximately 11–39% and 12–57% for the single-storey and two-storey structure models, respectively. It should also be noted that only peak lateral accelerations are compared, which may result in such large intervals in reduction levels. When full time-acceleration records are compared, the reduction level due to application of the PBs varies from 35% to more than 50%.

As expected, the reduction level strongly depends on the amplitude–frequency characteristics of the ground motion. More specifically, the smaller the difference between the predominant frequency of the ground motion and the natural frequency of the tested model structure, the lower the reduction level. Furthermore, it should also be underlined that the amplitude–frequency characteristics of mining tremors are quite different from those that are observed in the case of seismic events. Earthquake excitations are generally characterized by high amplitudes and predominant frequencies varying usually from 1 to 5 Hz, whereas mining tremors exhibit lower amplitudes but slightly higher predominant excitation frequencies, which are usually around 5 Hz or higher. Moreover, different earthquakes themselves are also characterized by different frequency content. This is the reason why the reduction in lateral accelerations is so different for various seismic excitations. For example, in the case of the single-storey structure model, the reduction in the peak acceleration is only 11.3% for the Northridge earthquake, while it is as large as 40.2% for the Loma Prieta earthquake (see Table 1). A similar situation also concerns the results of the seismic tests for the two-storey structure model, which has substantially different dynamic properties compared to the single-storey structure model. In this case, the smallest reduction in the peak acceleration (equal to 28.1%) has been obtained for the Loma Prieta earthquake, while the largest one (as large as 56.8%) has been observed for the San Fernando earthquake (see Table 2). Nevertheless, the results obtained explicitly confirm high effectiveness of the prototype PBs in reducing structural vibration during seismic excitations as well as mining tremors.

6. Conclusions

The present paper reports the results of the comprehensive experimental investigation designed to verify the effectiveness of a prototype base isolation system made of PBs in reducing structural vibrations. In order to get an insight into the basic mechanical characteristics of the polymer used,

material testing was firstly performed. The results clearly demonstrated that the analyzed polymer is markedly nonlinear and its mechanical behaviour strongly depends on the strain rate. Moreover, a relatively high value of the loss factor was obtained from the DMA tests, which confirms high damping properties of the material.

The next stage of the study was to conduct sine sweep tests to analyze the dynamic behaviour of the structure models with and without the PBs. As expected, the results obtained from the sine sweep tests confirmed that application of the prototype PBs leads to a significant decrease in the acceleration values experienced by the tested models during sinusoidal excitation. Peak accelerations were reduced by approximately 58% (from 7.74 to 3.25 m/s^2) and 45% (from 4.42 to 2.44 m/s^2) for the single-storey and two-storey structure models, respectively.

In the final stage of the current investigation, the structure models, both fixed-base and base-isolated, were subjected to the El Centro earthquake of 1940, the San Fernando earthquake of 1971, the Loma Prieta earthquake of 1989, the Northridge earthquake of 1994, and finally the Polkowice (Poland) tremor of 2002 as an example of mining-induced seismicity. The shaking table tests confirmed very high effectiveness of the isolation devices in improving dynamic behaviour of the experimental models. Peak lateral accelerations recorded at the top of the tested structures were reduced by approximately 11–39% and 12–57% for the single-storey and two-storey structure models, respectively. The results obtained clearly demonstrate that, due the application of the prototype base isolation system made of PBs, the peak lateral accelerations recorded at the top of the tested structures were markedly reduced. Additionally, it should be underlined that the horizontal displacement capacity of the PBs has not been exceeded under any tested earthquake excitation, which also confirms proper design of seismic bearings.

The results of the current study confirmed relatively high effectiveness of the prototype PBs in reducing structural vibrations of two experimental models. Nevertheless, there is a need for further development of the seismic isolation system based on the application of polymeric material. The studies are necessary to be conducted so as to fully verify the effectives of a full-scale multi-dimensional PBs as a base isolation system for real structures. These should include numerical simulations as well as experimental tests conducted on a large six degrees-of-freedom shaking table.

Acknowledgments: The authors are grateful to Arkadiusz Kwiecień and Bogusław Zając (Faculty of Civil Engineering, Cracow University of Technology, Poland) for preparing the polymeric specimens, which were used to construct the PBs considered in this research. In addition, the authors would like to thank Michał Strankowski and Łukasz Piszczyk (Chemical Faculty, Gdansk University of Technology, Poland) for their help in conducting the DMA tests.

Author Contributions: Tomasz Falborski and Robert Jankowski conceived, designed and performed the experimental investigation; Tomasz Falborski analyzed the data and wrote the paper; Both authors discussed the results obtained and commented on the paper at all stages.

Conflicts of Interest: The authors declare no conflict of interest.

References

1. Jankowski, R.; Mahmoud, S. *Earthquake-Induced Structural Pounding*; Springer: Cham, Switzerland, 2015.
2. Jankowski, R.; Mahmoud, S. Linking of adjacent three-storey buildings for mitigation of structural pounding during earthquakes. *Bull. Earthq. Eng.* **2016**, *14*, 3075–3097. [CrossRef]
3. Naderpour, H.; Barros, R.C.; Khatami, S.M.; Jankowski, R. Numerical study on pounding between two adjacent buildings under earthquake excitation. *Shock Vib.* **2016**, 1504783. [CrossRef]
4. Jankowski, R. Pounding between superstructure segments in multi-supported elevated bridge with three-span continuous deck under 3D non-uniform earthquake excitation. *J. Earthq. Tsunami* **2015**, *9*, 1550012. [CrossRef]
5. Ebrahimian, M.; Todorovska, M.I.; Falborski, T. Wave Method for Structural Health Monitoring: Testing Using Full-Scale Shake Table Experiment Data. *J. Struct. Eng.* **2016**, *143*. [CrossRef]
6. Elwardany, H.; Seleemah, A.; Jankowski, R. Seismic pounding behavior of multi-story buildings in series considering the effect of infill panels. *Eng. Struct.* **2017**, *144*, 139–150. [CrossRef]

7. Booth, E.; Key, D. *Earthquake Design Practice for Buildings*; Thomas Telford Publishing: London, UK, 2006.
8. Chopra, A.K. *Dynamics of Structures: Theory and Applications to Earthquake Engineering*; Prentice Hall: Englewood Cliffs, NJ, USA, 2012.
9. Housner, G.W.; Bergman, L.A.; Caughey, T.K.; Chassiakos, A.G.; Claus, R.O.; Masri, S.F.; Skelton, R.E.; Soong, T.T.; Spencer, B.F.; Yao, J.T.P. Structural control: Past, present, and future. *J. Eng. Mech.* **1997**, *123*, 897–971. [CrossRef]
10. Pasala, D.T.R.; Sarlis, A.A.; Nagarajaiah, S.; Reinhorn, A.M.; Constantinou, M.C.; Taylor, D. Adaptive negative stiffness: New structural modification approach for seismic protection. *J. Struct. Eng.* **2012**, *193*, 1112–1123. [CrossRef]
11. Spencer, B.F.; Nagarajaiah, S. State of the Art of Structural Control. *J. Struct. Eng.* **2003**, *129*, 845–856. [CrossRef]
12. Wolff, E.D.; Ipek, C.; Constantinou, M.C.; Tapan, M. Effect of viscous damping devices on the response of seismically isolated structures. *Earthq. Eng. Struct. Dyn.* **2015**, *44*, 185–198. [CrossRef]
13. Buckle, I.G. Passive control of structures for seismic loads. In Proceedings of the 12th World Conference on Earthquake Engineering, Auckland, New Zealand, 30 January–4 February 2000.
14. Robinson, W.H. Passive control of structures: The New Zealand experience. *J. Earthq. Technol.* **1998**, *35*, 63–75.
15. Aiken, I.D.; Nims, D.K.; Whittaker, A.S.; Kelly, J.M. Testing of passive energy dissipation systems. *Earthq. Spectra* **1993**, *9*, 335–370. [CrossRef]
16. Symans, M.D.; Constantinou, M.C. Semi-active control systems for seismic protection of structures: A state-of-the-art review. *Eng. Struct.* **1999**, *21*, 469–487. [CrossRef]
17. Kelly, J.M. Base isolation: Linear theory and design. *Earthq. Spectra* **1990**, *6*, 223–244. [CrossRef]
18. Buckle, I.G.; Mayes, R.L. Seismic isolation: History, application, and performance: A world view. *Earthq. Spectra* **1990**, *6*, 161–201. [CrossRef]
19. Skinner, R.I.; Robinson, W.H.; McVerry, G.H. *An Introduction to Seismic Isolation*; John Wiley and Sons: New York, NY, USA, 1993.
20. Komodromos, P. *Seismic Isolation of Earthquake-Resistant Structures*; WIT Press: Southampton, UK, 2000.
21. Naeim, F.; Kelly, J.M. *Design of Seismic Isolated Structures: From Theory to Practice*; John Wiley and Sons: New York, NY, USA, 1999.
22. Mahmoud, S.; Jankowski, R. Pounding-involved response of isolated and non-isolated buildings under earthquake excitation. *Earthq. Struct.* **2010**, *1*, 231–252. [CrossRef]
23. Kelly, J.M. *Earthquake-Resistant Design with Rubber*; Springer: London, UK, 1993.
24. Skinner, R.I.; Kelly, J.M.; Heine, A.J. Hysteretic dampers for earthquake-resistant structures. *Earthq. Eng. Struct. Dyn.* **1975**, *3*, 287–296. [CrossRef]
25. Robinson, W.H.; Greenbank, L.R. An extrusion energy absorber suitable for the protection of structures during an earthquake. *Earthq. Eng. Struct. Dyn.* **1976**, *4*, 251–259. [CrossRef]
26. Kumar, M.; Whittaker, A.S.; Constantinou, M.C. An advanced numerical model of elastomeric seismic isolation bearings. *Earthq. Eng. Struct. Dyn.* **2014**, *43*, 1955–1974. [CrossRef]
27. Tyler, R.G. Rubber bearings in base-isolated structures: A summary paper. *Bull. N. Z. Natl. Soc. Earthq. Eng.* **1991**, *24*, 251–274.
28. Mavronicola, E.; Komodromos, P. On the response of base-isolated buildings using bilinear models for LRBs subjected to pulse-like ground motions: Sharp vs. smooth behaviour. *Earthq. Struct.* **2014**, *7*, 1223–1240. [CrossRef]
29. Kumar, M.; Whittaker, A.S.; Constantinou, M.C. Characterizing friction in sliding isolation bearings. *Earthq. Eng. Struct. Dyn.* **2015**, *44*, 1409–1425. [CrossRef]
30. Mokha, A.; Constantinou, M.C.; Reinhorn, A.M.; Zayas, V.A. Experimental study of friction-pendulum isolation system. *J. Struct. Eng.* **1991**, *117*, 1201–1217.
31. Tsopelas, P.; Constantinou, M.C.; Kim, Y.S.; Okamoto, S. Experimental study of FPS system in bridge seismic isolation. *Earthq. Eng. Struct. Dyn.* **1996**, *25*, 65–78. [CrossRef]
32. Fenz, D.M.; Constantinou, M.C. Behaviour of the double concave friction pendulum bearing. *Earthq. Eng. Struct. Dyn.* **2006**, *35*, 1403–1424. [CrossRef]

33. Nagarajaiah, S.; Xiaohong, S. Seismic performance of base-isolated buildings in the 1994 Northridge earthquake. In Proceedings of the 11th World Conference on Earthquake Engineering, Acapulco, Mexico, 23–28 June 1996.
34. Nagarajaiah, S.; Xiaohong, S. Response of base-isolated USC hospital building in Northridge earthquake. *J. Struct. Eng.* **2000**, *126*, 1177–1188. [CrossRef]
35. Falborski, T.; Jankowski, R.; Kwiecień, A. Experimental study on polymer mass used to repair damaged structures. *Key Eng. Mater.* **2012**, *488*, 347–350. [CrossRef]
36. Zembaty, Z. Rockburst induced ground motion-a comparative study. *SDEE* **2004**, *24*, 11–23. [CrossRef]